

Monte Carlo study of electron transport in strained silicon inversion layers

E. Ungersboeck · H. Kosina

© Springer Science + Business Media, LLC 2006

Abstract The effect of degeneracy both on the phonon-limited mobility and the effective mobility including surface-roughness scattering in unstrained and biaxially tensile strained Si inversion layers is analyzed. We introduce a new method for the inclusion of the Pauli principle in a Monte Carlo algorithm. We show that incidentally degeneracy has a minor effect on the bulk effective mobility, despite non-degenerate statistics yields unphysical subband populations and an underestimation of the mean electron energy. The effective mobility of strained inversion layers slightly increases at high inversion layer concentrations when taking into account degenerate statistics.

Keywords Monte Carlo simulation · Degeneracy effects · Strain · Mobility enhancement

1. Introduction

During the last years the introduction of strain in the channel of Si MOSFETs has become a widely used technique to improve transistor drive currents [1–3]. Strain can be induced by epitaxially growing thin Si layers on relaxed $\text{Si}_{1-y}\text{Ge}_y$ substrates, or alternatively, by processing additional cap layers over the transistors. The latter method is especially suitable for mass production because it requires only a slight modification of the process flow [4].

Surprisingly, from a theoretical viewpoint the mobility enhancement caused by strain is still an issue of discussion. The reason for this is manifold: It was claimed that using

the well established models for scattering in the two dimensional electron gas (2DEG) the mobility gain of strained Si (SSi) at low effective fields should be compensated by more pronounced surface roughness scattering at large effective fields [5]. Due to this fact, only with the assumption of much smoother strained Si-SiO₂ interfaces one should be able to get qualitative agreement with experimental data. Even though it seemed to be unphysical to change the smoothness of the strained Si-SiO₂ interface, the Monte Carlo (MC) community has adopted this assumption [6] or simply not responded to the troubling fact.

When trying to clarify this dissatisfactory status two main difficulties arise: First, there exists a variety of surface roughness scattering models, and it is not clear which approximations to the general expression given by Ando [7] are allowed. Second, there is a discordance whether and how degeneracy effects should be included in transport calculations of inversion layers.

In this paper, the ways to include the Pauli principle in a MC algorithm are revised and critically compared to each other. The usual method, where the Pauli blocking factor $1 - f(\mathbf{k})$ is approximated using the equilibrium distribution function $f_{\text{FD}}(\mathbf{k})$, can be shown to lead to unphysical subband populations, kinetic energies, and mobilities. The reason being that at high degeneracy the error $\varepsilon(\mathbf{k}) = f(\mathbf{k}) - f_{\text{FD}}(\mathbf{k})$ is dominant. A new MC algorithm accounting for the Pauli exclusion principle is proposed which is less sensitive to the error $\varepsilon(\mathbf{k})$.

The paper is organized as follows: Section 2 describes the new approach to implement the Pauli exclusion principle in the MC method. It is shown that in the low field limit the proposed algorithm yields the same mobility as the Kubo Greenwood formula, while other algorithms do not. We use the new method to extract velocity profiles and illustrate the large effect of degeneracy on the electron system. Finally,

E. Ungersboeck (✉) · H. Kosina
Institut für Mikroelektronik, Vienna University of Technology,
TU Wien, Gusshausstrasse 27–29, A-1040 Vienna, Austria
e-mail: ungersboeck@iue.tuwien.ac.at

the simulated effective mobility curves for unstrained and biaxially tensile strained Si on relaxed Si_{1-y}Ge_y substrates are presented in Section 3.

2. Inclusion of the Pauli principle in Monte Carlo simulations

In transport calculations of the 2DEG forming in the channel of MOSFETs the inclusion of the Pauli principle is expected to be important since the lowest subband may lie well below the Fermi level in the regime of moderate and high effective fields (high inversion layer concentrations). This leads to modified subband populations and an elevated mean kinetic energy of electrons as compared to the nondegenerate case. A change in the mobility is therefore to be expected.

The proposed algorithm is based on the following reformulation of the degenerate scattering operator.

$$\begin{aligned} Q[f]_{\mathbf{k}} &= \int f_{\mathbf{k}'}(1 - f_{\mathbf{k}})S_{\mathbf{k}',\mathbf{k}} d\mathbf{k}' - \int f_{\mathbf{k}}(1 - f_{\mathbf{k}'})S_{\mathbf{k},\mathbf{k}'} d\mathbf{k}' \\ &= \int f_{\mathbf{k}'}S_{\mathbf{k}',\mathbf{k}} - f_{\mathbf{k}}S_{\mathbf{k},\mathbf{k}'} + \underbrace{f_{\mathbf{k}}f_{\mathbf{k}'}(S_{\mathbf{k},\mathbf{k}'} - S_{\mathbf{k}',\mathbf{k}})}_{\text{additional term}} d\mathbf{k}'. \end{aligned}$$

The last term represents a nonlinear correction to the non-degenerate scattering operator. To linearize the scattering operator it is common to keep one factor of the product $f_{\mathbf{k}}f_{\mathbf{k}'}$ constant and to treat the other as the unknown.

Near thermodynamic equilibrium, f can be approximated by the Fermi-Dirac distribution function f_{FD} . The key point of the new method is that a symmetric approximation with respect to \mathbf{k} and \mathbf{k}' is employed.

$$f(\mathbf{k})f(\mathbf{k}') \approx \frac{1}{2}(f(\mathbf{k})f_{\text{FD}}(\mathbf{k}') + f_{\text{FD}}(\mathbf{k})f(\mathbf{k}')) \quad (1)$$

Using this approximation the scattering operator can be expressed in terms of a modified transition rate $\widehat{S}_{\mathbf{k},\mathbf{k}'}$ and scattering rate $\widehat{\lambda}_{\mathbf{k}}$ as

$$Q[f]_{\mathbf{k}} = \int f(\mathbf{k}')\widehat{S}_{\mathbf{k}',\mathbf{k}} d\mathbf{k}' - f(\mathbf{k})\widehat{\lambda}_{\mathbf{k}}.$$

with

$$\widehat{S}_{\mathbf{k},\mathbf{k}'} = S_{\mathbf{k},\mathbf{k}'} \left(1 - \frac{1}{2}f_{\text{FD}}(\mathbf{k}')\right) + S_{\mathbf{k}',\mathbf{k}} \frac{1}{2}f_{\text{FD}}(\mathbf{k}') \quad (2)$$

$$\widehat{\lambda}_{\mathbf{k}} = \int \widehat{S}_{\mathbf{k},\mathbf{k}'} d\mathbf{k}' \quad (3)$$

A simple error analysis shows the advantage of this formulation. Consider a highly degenerate state \mathbf{k} , characterized by $f(\mathbf{k}) \approx 1$. A direct approximation of the blocking factor

$(1 - f(\mathbf{k}))$ can give completely wrong results, because the approximation of the blocking factor is determined by the error, $1 - (f_{\text{FD}} + \varepsilon) \approx \varepsilon$. In the formulation (2), however, because of $\varepsilon \ll 1$ the effect of the error will be negligible, $1 - (f_{\text{FD}} + \varepsilon)/2 \approx 1/2$.

The modified transition rate (2) is given by a linear combination of the forward rate $S_{\mathbf{k},\mathbf{k}'}$ and backward rate $S_{\mathbf{k}',\mathbf{k}}$. The latter can be expressed in terms of the forward rate by means of the principle of detailed balance. The modified scattering rates for phonon emission and absorption become,

$$\begin{aligned} \widehat{\lambda}_{em} &= \lambda_{em} \cdot \left(1 - \frac{1}{2} \frac{f_{\text{FD}}(\varepsilon_f)}{N_0 + 1}\right) \\ \widehat{\lambda}_{ab} &= \lambda_{ab} \cdot \left(1 + \frac{1}{2} \frac{f_{\text{FD}}(\varepsilon_f)}{N_0}\right), \end{aligned}$$

where ε_f denotes the final energy and N_0 the equilibrium phonon distribution function,

$$N_0 = \frac{1}{\exp\left(\frac{\hbar\omega_0}{k_B T}\right) - 1}.$$

For elastic scattering mechanisms the modified scattering rates do not change from the classical ones, $\widehat{\lambda}_{\mathbf{k}} = \lambda_{\mathbf{k}}$. In the simulation of the 2DEG to a good approximation one can assume scattering with surface roughness, impurities, and acoustical phonons to be elastic.

To implement the Pauli principle in a conventional MC program for non-degenerate statistics the only modifications necessary are the replacement of the classical scattering rates by the modified ones.

2.1. Comparison of algorithms

The new algorithm has been compared to two other methods found in the literature [8, 9]. The first algorithm to include the Pauli principle in the MC technique [8] is based on a self-consistent iterative algorithm that uses a rejection technique to account for the occupation probability of the final state at each scattering event. Since this auxiliary self-scattering mechanism is proportional to the occupation of the final states, the algorithm prevents a large number of classically allowed transitions.

A different approach to include degeneracy in MC simulations was given in [9]. Inelastic scattering rates are multiplied with a factor of $(1 - f_{\text{FD}}(\varepsilon_f))/(1 - f_{\text{FD}}(\varepsilon_i))$, where ε_i (ε_f) denotes the initial (final) electron energy. This additional factor stems from the use of Fermi-Dirac statistics within the relaxation time approximation [10].

In the limit of vanishing field the mobility can also be calculated using the relaxation time approximation. Thus we compare our MC algorithm and a modified method

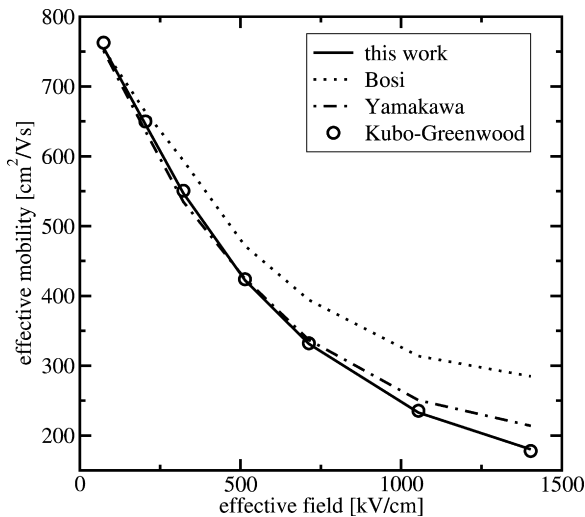


Fig. 1 The simulated effective mobility using the new algorithm (solid line) is compared to results of a non-selfconsistent version of Bosi’s algorithm [8] (dotted line), the algorithm proposed by [9], and to the mobility calculated with the Kubo-Greenwood formalism (open circles)

from [8] and [9] to the mobility calculated from the Kubo-Greenwood expression [11]. From Fig. 1 it can be seen that the new method yields the closest agreement, whereas a non-selfconsistent implementation of the algorithm proposed in [8], where $f(\mathbf{k})$ has been approximated by the equilibrium distribution function $f_{FD}(\mathbf{k})$, and the algorithm proposed by [9] overestimate the effective mobility.

3. Results

We extract the mean electron velocity as a function of total electron energy in the small-field limit, by recording the velocity component along the driving field as a function of the total electron energy. For this purpose the particles energy domain was divided into a set of intervals $\Delta\mathcal{E}$. The mean velocity of an electron in a particular interval $\mathcal{E}_0 \leq \mathcal{E} \leq \mathcal{E}_0 + \Delta\mathcal{E}$ can be obtained during a MC simulation from a history of duration T

$$\bar{v}(\mathcal{E}_0) = \frac{1}{T} \int_0^T v[\mathbf{k}(t)] \times (\theta[\mathcal{E}(t) - \mathcal{E}_0] - \theta[\mathcal{E}(t) - \mathcal{E}_0 - \Delta\mathcal{E}]) dt, \tag{4}$$

where $\theta(\mathcal{E})$ denotes the step function and $\mathbf{k}(t)$ represents the electron wave vector during the flight. Note that the overall mobility is proportional to the sum of the mean velocities of all intervals.

A very interesting behavior can be observed when comparing the mean velocities resulting from simulations with classical and Fermi-Dirac statistics. The upper plot of Fig. 2 shows that when considering only phonon scattering the

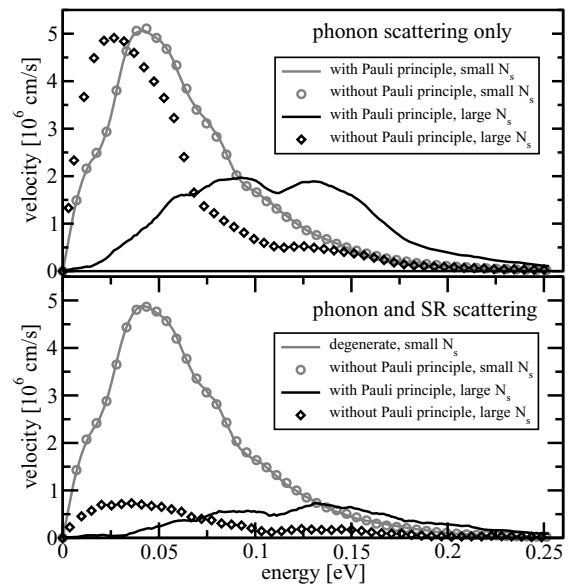


Fig. 2 Mean velocities resulting from simulations with (lines) and without (symbols) inclusion of the Pauli principle for an inversion layer density $N_s \approx 10^{11} \text{ cm}^{-2}$ (grey) and $N_s \approx 1.5 \times 10^{13} \text{ cm}^{-2}$ (black)

mean velocities coincide for both simulation modes in the non-degenerate regime ($E_f - E_0 \approx -0.13 \text{ eV}$). At high inversion layer concentrations, where the 2DEG is highly degenerate ($E_f - E_0 \approx 0.8 \text{ eV}$), a shift of the mean velocity distribution toward higher energies and a decrease of its peak can be observed as compared to the mean velocity resulting from simulations without the Pauli principle. The coincidence of the mean velocities in the non-degenerate regime is merely a test that the algorithm with the Pauli principle included converges to the classical algorithm for the non-degenerate 2DEG. At high inversion layer concentrations the different mean velocities can be interpreted as follows: In simulations neglecting the Pauli principle electrons will have an equilibrium energy of $k_B T$ whereas the mean energy resulting from simulations with the Pauli principle can be more than twice as much. Since phonon scattering is merely proportional to the density of states, which is an increasing step-like function in the 2DEG, electrons being at higher energies—as it is the case in simulations with the Pauli principle—experience more scattering and thus the phonon-limited mobility is strongly decreased (see Fig. 3).

The lower plot of Fig. 2 shows the mean velocities when surface roughness scattering has been included in simulations. In the low inversion layer density regime (depicted in grey) surface roughness scattering does not play an important role, and the mean velocities compare well with the simulation results with only phonon scattering included. Interestingly now even at high inversion layer densities the mean velocities (depicted in black) stemming from simulations with and without the Pauli principle do not differ as much. The large peak in the mean velocity

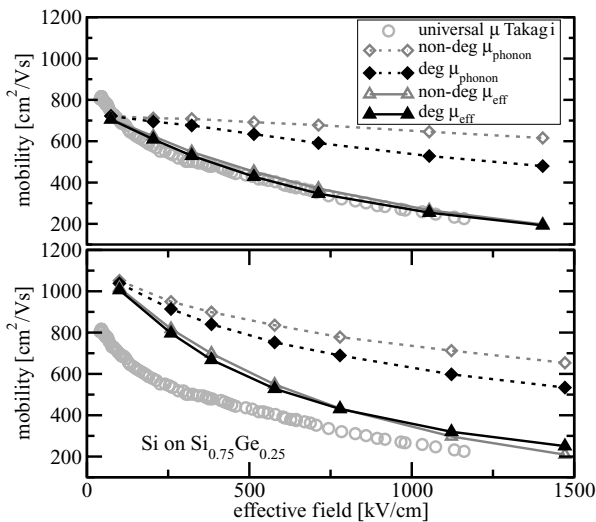


Fig. 3 Calculated phonon-limited and effective mobility compared to the universal mobility curve with and without degeneracy effects for unstrained Si (upper curve) and biaxially strained Si (lower curve)

at small energies that could be observed in simulations including only phonon scattering but neglecting the Pauli principle is here suppressed. This stems from the influence of surface roughness scattering which is more effective at small energies in contrast to phonon scattering.

Finally from Fig. 2 one can also observe that due to degeneracy effects electrons at energies below the Fermi level have smaller velocities which corresponds to the general picture that these electrons have little contribution to transport.

The new algorithm is used to extract the effective mobility in unstrained and biaxially tensile strained Si inversion layers. For the simulations a one-dimensional Schrödinger-Poisson solver [12] is used with modifications to account for the energy splitting between the twofold and the fourfold conduction-band minima and for the change of the band-gap [5]. From these results the matrix elements for phonon and surface roughness scattering and the form factors are calculated following [13]. Screening of the surface roughness scattering was included according to [13] while impurity scattering has been ignored as we mainly focus on the high-density (high effective field) region. The dielectric function was treated as a tensor quantity and not as a scalar function as the latter approximation is only valid for ideal 2D systems where the wave functions have a δ -like shape. Furthermore the plasma dispersion function was not used to calculate the polarization function, as the plasma dispersion function underestimates the polarization function in the degenerate case. A non-parabolic bandstructure ($\alpha = 0.5 \text{ eV}^{-1}$) was used leading to a 20% reduction of the phonon-limited mobility at 300 K in agreement with [5]. For

all simulations presented here a uniform doping concentration of $2 \times 10^{16} \text{ cm}^{-3}$ has been assumed.

The simulated mobility curve for unstrained Si in the upper plot of Fig. 3 shows good agreement with the universal mobility curve by Takagi [14]. Surprisingly, the effective mobility resulting from simulations with degenerate statistics are in close agreement to those using classical statistics even though the phonon-limited mobility experiences a noticeable reduction when using degenerate statistics. As previously discussed, this close agreement can only be understood from the cancellation of two effects: Degeneracy leads to an increase of the mean kinetic energy. This leads to an increase in phonon scattering and a decrease in the mobility. At the same time electrons with larger kinetic energies experience less effective surface-roughness scattering, thus the surface roughness limited mobility is increased. In unstrained Si by chance these two effects cancel each other at all effective fields, and the difference between a simulation with non-degenerate and degenerate statistics is very small.

Having calibrated our model against the unstrained universal mobility curve, a simulation of biaxially strained Si on relaxed $\text{Si}_{1-y}\text{Ge}_y$ substrates with $y = 0.25$ was performed. From Fig. 3 it can be observed that in SSi inversion layers, where the ratio between phonon and surface roughness scattering is different—due to suppressed intervalley transitions—simulations with degeneracy effects yield higher mobilities $\mu_{\text{sr,deg}} > \mu_{\text{sr,nondeg}}$.

Our simulation results for the inversion layer mobility in biaxially strained Si on $\text{Si}_{1-y}\text{Ge}_y$ for various Ge contents suggest a saturation of the mobility enhancement at $y \approx 25\%$. As can be seen from Fig. 3 the anomalous intersection of the strained and unstrained mobility curve from [5] was not

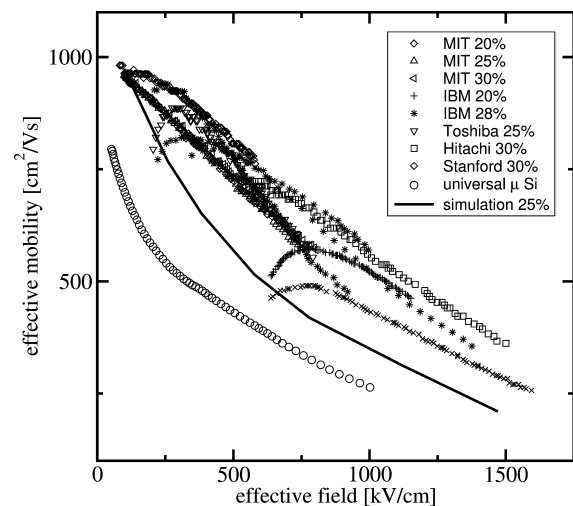


Fig. 4 Comparison of simulations results for the effective mobility of biaxially strained Si on $\text{Si}_{1-y}\text{Ge}_y$ with $y = 0.25$ with published data from different experimental groups for various substrate compositions of Ge

observed, however Fig. 4 indicates that the predicted mobility for SSi is still underestimated.

4. Conclusions

By means of MC simulations we are able to deduce the effect of degeneracy both on the phonon-limited mobility and the effective mobility including surface-roughness scattering. It is shown that in the unstrained case the inclusion of the Pauli principle leads to a noticeable reduction of the phonon-limited mobility, but has almost no impact on the effective mobility. The effective mobility of strained inversion layers increases slightly at high inversion layer concentrations when taking into account degenerate statistics. Thus a correct treatment of degenerate carrier statistics of the 2DEG of strained Si inversion layers is important.

However, this study cannot explain the experimental mobility enhancement for SSi, which is still underestimated at large effective fields, where surface roughness scattering dominates. Thus a careful revision of surface roughness scattering might be needed to achieve the correct mobility enhancements.

Acknowledgment This work has been partly supported by the European Commission, project SINANO, IST 506844.

References

1. L.-J. Huang, J. Chu, S. Goma, C. Emic, S. Koester, D. Canaperi, P. Mooney, S. Cordes, J. Speidell, R. Anderson, and H. Wong, in *VLSI Symp. Tech. Dig.*, (2001), pp. 57–58.
2. K. Rim, J. Chu, H. Chen, K. Jenkins, T. Kanarsky, K. Lee, A. Mocuta, H. Zhu, R. Roy, J. Newbury, J. Ott, K. Petrarca, P. Mooney, D. Lacey, S. Koester, K. Chan, D. Boyd, M. Jeong, and H. Wong, in *VLSI Symp. Tech. Dig.*, (2002), pp. 98–99.
3. N. Sugii, D. Hisamoto, K. Washio, N. Yokoyama, and S. Kimura, in *Intl. Electron Devices Meeting*, (2001), pp. 737–740.
4. S.-E. Thompson, M. Armstrong, C. Auth, M. Alavi, and M. Buehler, *IEEE Trans. Electron Devices*, **51**, 1790 (2004).
5. M. V. Fischetti, F. Gamiz, and W. Hänsch, *J. Appl. Phys.*, **92**, 7320 (2002).
6. J. Watling, L. Yang, M. Borici, R. C. Wilkins, A. Asenov, J. R. Barker, and S. Roy, *Solid-State Electron.*, **48**, 1337 (2004).
7. T. Ando, A. Fowler, and F. Stern, *Review of Modern Physics*, **54**, 437 (1982).
8. S. Bosi and C. Jacoboni, *J. Physics C*, **9**, 315 (1976).
9. S. Yamakawa, H. Ueno, K. Taniguchi, C. Hamaguchi, K. Miyatsuji, K. Masaki, and U. Ravaioli, *J. Appl. Phys.*, **79**, 911 (1996).
10. D. Roychoudhury and P. K. Basu, *Physical Review, B*, **22**, 6325 (1980).
11. M. V. Fischetti and Z. Ren, *J. Appl. Phys.*, **94**, 1079 (2003).
12. D. Vasileska, and Z. Ren, *SCHRED 2.0 User's Manual*, <http://www.nanohub.org>, (2000).
13. C. Jungemann, A. Edmunds, and W. Engl, *Solid-State Electron.*, **36**, 1529 (1993).
14. S. Takagi, A. Toriumi, M. Iwase, and H. Tango, *IEEE Trans. Electron Devices*, **41**, 2357 (1994).